Pharmaceutical Research, Vol. 25, No. 5, May 2008 (© 2007)
DOI: 10.1007/s11095-007-9506-y

Research Paper

Structural Behaviour of 2-Hydroxypropyl-β-Cyclodextrin in Water: Molecular Dynamics Simulation Studies

Chin Weng Yong,[1,3] Clive Washington,[2] and William Smith[1]

Received June 29, 2007; accepted November 19, 2007; published online December 28, 2007

Purpose. To investigate the effect of 2-hydroxypropyl side group substitutions on the structure of β-cyclodextrin (CD) in water.
Methods. Molecular dynamics simulations were carried out on four HPBCDs that broadly represent a range of degree of substitutions in order to investigate the effect of substitution of β-cyclodextrin with 2-hydroxypropyl groups at various O2 and O6 positions of the glucose units.
Results. The 2-hydroxypropyl side groups located at the O2 positions widen the cavity entrance at the secondary OH position of the CD molecule. These groups are spatially more spread out but dynamically more restricted, due to the formation of a hydrogen bond network between the hydroxyl groups of the side chains and the glucose units. On the other hand, the 2-hydroxypropyl groups at the O6 positions are dynamically more flexible.
Conclusions. The extent and the location of the substitution can affect the cavity structure of the CD molecule, and thus possibly the molecular encapsulation capabilities.

KEY WORDS: β-cyclodextrin derivatives; hydrogen bonding; 2-hydroxypropyl; molecular dynamics; water interaction.

INTRODUCTION

Cyclodextrins (CD) are cyclic oligosaccharides which consist of at least six glucose units linked by α 1–4 glycosidic bonds. They are readily available from the enzymatic hydrolysis of starch. Cyclodextrins that are made of six membered (α), seven membered (β) and eight membered (γ) glucose units have near-perfect circular shape, adopting an approximately truncated cylindrical conical form. Figure 1a illustrates the linkage of two glucose units in a typical cyclodextrin molecule. The orientation of the individual glucose units are such that the primary hydroxyl groups at the C6 positions outline the narrow rim of the truncated cone, while the secondary hydroxyl groups at the C2 and C3 positions outline the wider rim of the truncated cone. As a result, the walls of the cavity are lined with hydrophobic hydrogen atoms at the C3 and C5 positions. Note that this orientation also allows an intramolecular hydrogen bonding network (O2–O3) to form between the hydroxyl groups located at the C2 and C3 positions respectively. Figure 1b shows a typical molecular structure of a CD and the schematic projection of its conical structure. The hydrogen atoms have been omitted for clarity. In addition to the circular shape, the aperture angle of the conical structure also influences the shape of the cavity. This tilt angle can be defined as the angle τ between the plane containing the glycosidic O4 atoms (labelled as blue spheres in Fig. 1b and the plane of a glucose unit. A smaller average τ value corresponds to a conical shape, whereas a value of 90° gives a perfect cylindrical shape. A value larger than 90° indicates an inverted conical structure.

The cavity of β-CD is suitable for the complexation of a wide range of small drug molecules. Unfortunately, this molecule is in itself of low water solubility, and displays nephrotoxicity. These problems are alleviated by chemically modifying the β-CD through substitution of the hydroxyl groups at various positions. Among the various CD derivatives, the 2-hydroxypropyl-β-CD (2-HPBCD) (4–6) is considered to be most useful, due to its high solubility in water and low toxicity. For these reasons, substituted cyclodextrins have a wide range of important applications in pharmaceutical, food science and cosmetic industries (1,2). In the former field, cyclodextrins have been mainly used in inclusion complexation to increase solubility, stability and to reduce the toxicity of drug molecules. Therefore, they have potential use in enhancing the efficiency of drug delivery systems (3).

A great deal of work has been carried out to study interactions between water and un-substituted CDs. Experimentally, water interaction behaviour is obtained indirectly from crystal studies (7,8) and spectroscopic methods such as NMR (9). In the case of theoretical studies, interactions of isolated water molecules and CDs have been carried out quan-

[1] Computational Science and Engineering Department, Daresbury Laboratory, STFC, Daresbury, Warrington WA4 4AD, UK.
[2] AstraZeneca, PU8 Lab Block, Macclesfield Works, Hurdsfield Industrial Estate, Macclesfield SK10 2NA, UK.
[3] To whom correspondence should be addressed. (e-mail: c.w.yong@dl.ac.uk)

ABBREVIATIONS: CD, cyclodextrin; 2-HPBCD, 2-hydroxypropyl-β-cyclodextrin.

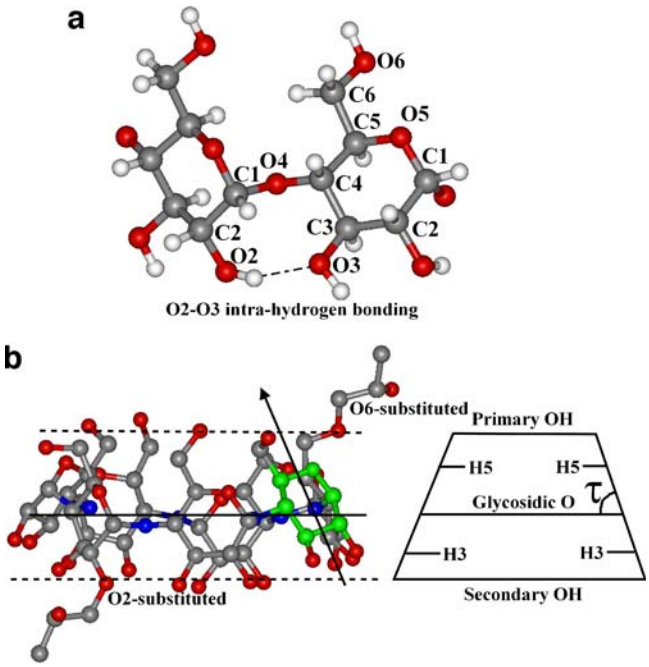

Fig. 1. Illustration of cyclodextrin atomic structure: **a** repeating unit of two glucose showing the intramolecular hydrogen bonding. **b** Definition of atom groups.

tum mechanically (10,11). However, CDs in aqueous solutions are known to exhibit complex hydrogen bond networks. Therefore, computational methods such as molecular dynamics are particularly suited to study detailed water interactions and the corresponding CD molecular structural behaviour at an atomistic level. Such knowledge may be important in understanding the fundamental aspects of inclusion mechanisms, for instance competitive interactions between hydrophobic guest molecules and water molecules within the CD cavity bound by hydrogen bonds. The vast majority of published computational works are concerned with the un-substituted CDs (12–16). Despite the commercial importance of substituted CDs, such as 2-HPBCD, there are hardly any published molecular simulation studies in the literature.

In this paper, we present molecular dynamics simulations of the fully-solvated 2-HPBCD. Unfortunately, as in the case of other chemically-modified CDs, a precise structural description of 2-HPBCD is very difficult. This is due to the wide range of substitution patterns occurring during the derivitization, and the difficulty of separating individual derivatives and isomers from one another. For this reason, commercial samples are often sold in the form of a 2-HPBCD mixture with a certain range of degree of substitution (DS) (17). The 2-HPBCDs are usually produced via a condensation reaction between the β-CD and propylene oxide in alkaline solution. The position of substitution can be partially controlled by varying the alkalinity. For instance, low alkalinity results in substitution at the O2 positions, whereas high alkalinity results in substitution at the O6 positions (4). Obviously, it would be impractical to model all possible combinations of 2-hydroxypropyl substituted CDs. In this work, we have selected two molecular species: 2-hydroxypropyl substitution only at all the O2 positions, and 2-hydroxypropyl substitution at all the O2 and O6 positions, as representations for 2-HPBCD mixtures that are produced in low and high alkalinity respectively. In addition, two more models were also considered, with only partial substitutions at the O2 and O6 positions (see below). Of note is that, in reality, substitutions always occur randomly and are distributed among the different glucose units at all concentrations, so the commercial materials are mixtures of very large numbers of isomers. However, we intend to make comparisons between the above-mentioned molecular species and the native β-CD molecule, in order to investigate the effects of substitution on the CD molecular structure in aqueous media. This may then provide a reference basis for making predictions of water interactions on other forms of 2-HPBCD isomers. In addition, we have also found that the exact nature of substitution can directly affect the affinity and selectivity of molecular encapsulation behaviour of the 2-HPBCD (Yong, *et. al.*, manuscript in preparation).

METHODS

The DL_POLY_2 program suite (18) was used to run the molecular dynamics simulations. Five fully solvated molecular models have been considered: the unmodified (native) β-CD, and four 2-hydroxypropyl derivatives, substituted to different extents at the O2 and O6 positions. The derivatives were chosen in order to represent a wide range of substitution patterns. The substitution patterns of these molecules are summarised in Table I. Each molecular model was placed at the centre of the simulation box of initial size 60×60×60 Å that contained pre-equilibrated TIP3P (19) water molecules at a density of 1.0 g/cm^3. Water molecules that overlapped with the CD molecules, or at a distance of less than 1.9 Å from the CD molecules, were removed. This gave a total of about 22000 atoms. The all-atom CHARMM22 force field (20) was used to model the atomic interactions and all atomic bonds were represented by flexible harmonic springs. The smoothed particle mesh Ewald method (21) was used to calculate the Coulombic long-range interactions. The Van der Waals short range cut off was set at 8 Å. A long-range correction was included in the force evaluation in order to take into account the residue interactions beyond the cut off limit. A fixed time step of 1.4 fs was used throughout the simulations.

We have tested the validity of our simulation model by making structural comparison (C. W. Yong, AstraZeneca internal report) of native α-CD and β-CD molecules between our simulation results and the experimental crystal structures (8). However, the conformational behaviour of cyclodextrin molecules is known to be rather different between the crystalline form and in aqueous medium (14). For this reason, we have also compared our models with a range of different α-

Table I. Model Summary

Models	O2 substitution	O6 substitution
β-CD	None	None
A	All	None
B	All	All
C	All	At glucose units 1, 3, 5 and 7
D	At glucose units 1, 3, 5 and 7	At glucose units 1, 3, 5 and 7

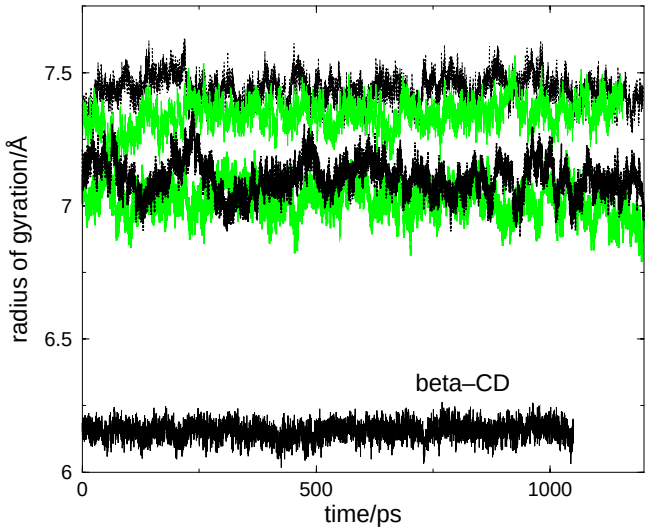

Fig. 2. The radii of gyration of cyclodextrin molecules. Model A: *green thick solid line*; Model B: *black thin dotted line*; Model C: *thin green solid line*; Model D: *black thick dotted line.*

CD and β-CD models including AMBER (16), CHARMM22 (implicit solvent) (22), AMBER-based Monte Carlo (23) and gas phase quantum mechanical calculations (23). The structural measurements are found to be in reasonably good agreement with crystal structures and other simulation models.

For the 2-HPBCD simulation model, the system was initially equilibrated in the NVE ensemble by monitoring the configuration energy. The system was considered to have reached an equilibrium state when the energy was found to fluctuate at a constant level, which occurred within 100 ps. This was subsequently switched to an NPT ensemble, and maintained at a temperature and pressure of 300 K and 1 atm respectively, using the Nosé–Hoover formalism (24). A further 100 ps simulation was carried out for equilibration before the sampling results were obtained over 1 ns.

RESULTS

Molecular Structure

Figure 2 compares the radii of gyration (R_g) of the various CD models. The results are a measure of the size of the molecule, representing the average spatial extent of the constituent atoms from the centre of gravity of the molecule. As would be expected, the radius of gyration increased as more hydroxypropyl groups were added. The greater variance in R_g for the substituted species compared to β-CD indicates an increase of molecular size fluctuations when the β-CD molecules were derivatised, due to an increase in the side group flexibility. Models B and C have rather similar values of R_g despite the fact that the latter model has a smaller degree of substitution, by about 40%, when compared with Model B. On the other hand, models A and D, which have a similar total number of substitutions, show similar values of the radii of gyration. The results seem to show that side chain substitution at the O2 position results in more "spread out" configurations than the substitution at the O6 position.

In order to determine the influence of the substitutions upon the CD cavity geometry, we can define a dimensionless shape factor for the cavity ring, as outlined by the glycosidic oxygen linkages, as follows

$$C = 1 - \frac{\sum_{i>j}^{3} (L_i - L_j)^2}{2\left(\sum_{i=1}^{3} L_i\right)^2} \quad (1)$$

where L_i are three sets of distances between a glycosidic oxygen atom and the mid-point between two opposing glycosidic oxygen atoms. It can be seen that C=1.0 when L_1=L_2=L_3, which means that the cavity has a perfect circular shape. When C becomes smaller, this means it is increasingly elongated, adopting an elliptical shape. Alternatively, the overall average shape of the CD molecule can be quantified from the principal radius of gyration tensor, λ, by defining a shape factor (asphericity), A as:

$$A = \frac{\sum_{i>j}^{3} (\lambda_i - \lambda_j)^2}{2\left(\sum_{i=1}^{3} \lambda_i\right)^2} \quad (2)$$

In this case, a smaller A value refers to a molecule tending towards a spherical form. Table II lists the structural measurements of the CD molecules studied. Examination of the variance of the L_i values shows that substituted CDs have larger fluctuations, although with rather similar average values of L when compared with those of native β-CD. There is a small decrease of only about 0.14% of the cavity shape when compared with that of native CD. This suggests that there is no significant change in the overall size of the cavity upon substitution. However, there is a noticeable increase of cavity shape fluctuation as a result of substitution.

The overall molecular shape values A decrease as the cyclodextrin molecule is substituted. Since the glucose ring structures remain essentially unchanged, the associated fluctuation values of A are therefore mainly due to the relatively flexible motion of the 2-hydroxypropyl side groups. For instance, Model A has the smallest fluctuation value (0.0089) among the substituted CDs, while Model D has the largest fluctuation of A (0.0154), although the degree of substitutions were the same for both models. On the other hand, fluctuation increases as the O6 groups were substituted (compare Model A with Model B and Model C). These results show that the side groups located at the primary alcohol O are more flexible than those located at the O2 positions.

Table II. Structural Measurements of the CD Molecules

Model	Average L/ Å	Circularity, C	Asphericity, A	τ/deg.
β-CD	9.544±0.093	0.9997±0.0004	0.1436±0.0042	82.7±2.7
A	9.575±0.134	0.9990±0.0008	0.1322±0.0089	75.9±2.7
B	9.498±0.108	0.9986±0.0013	0.0777±0.0098	78.2±2.6
C	9.616±0.122	0.9983±0.0017	0.1032±0.0105	76.7±2.9
D	9.653±0.116	0.9993±0.0007	0.0966±0.0154	78.9±2.8

The errors refer to the standard deviation of the average values.

Table II also shows that the average tilt angles τ of the glucose units for substituted CDs are smaller compared with those of β-CD. This results in widening of the cavity entrance at the secondary O side but narrowing of the cavity entrance at the primary O side. Analysis of the individual glucose units of the substituted CDs indicates that they adopt a wide range of tilt angles, in contrast to the native CD. This is shown in Fig. 3a for β-CD and Fig. 3b for Model A as an example. Note that only the results for the glucose units that adopt maximum and minimum tilt angles are shown for clarity purposes. The tilt angle results for other substituted CD models are not shown as they appear qualitatively similar to that of Model A.

The overall conical shapes of the substituted CDs are still preserved, although the tilting can swing either inward or outward with respect to the cavity. In general, it was noticed that substitutions at the O2 positions enhance the inward tilting (smaller τ angle) of the glucose units. This widens the cavity entrance as outlined by the O2 atoms but reduces the cavity thickness. For this reason, model A has the smallest value of τ. On the other hand, substitution at the O6 positions reduces the tilting effect to give a larger value of τ. For instance, full substitution at the O6 positions (model B) increases the tilt angle, but then it decreases slightly with partial substitution at the O6 positions (model C). Furthermore, reducing the number of substitutions at the O2 positions increase the value of τ again (model D). This shows that substitutions at the O2 and O6 positions play direct but counter roles in enhancing the rotation of a glucose unit about an axis joining two neighbouring glycosidic oxygen atoms, thus influencing the shape of the cavity.

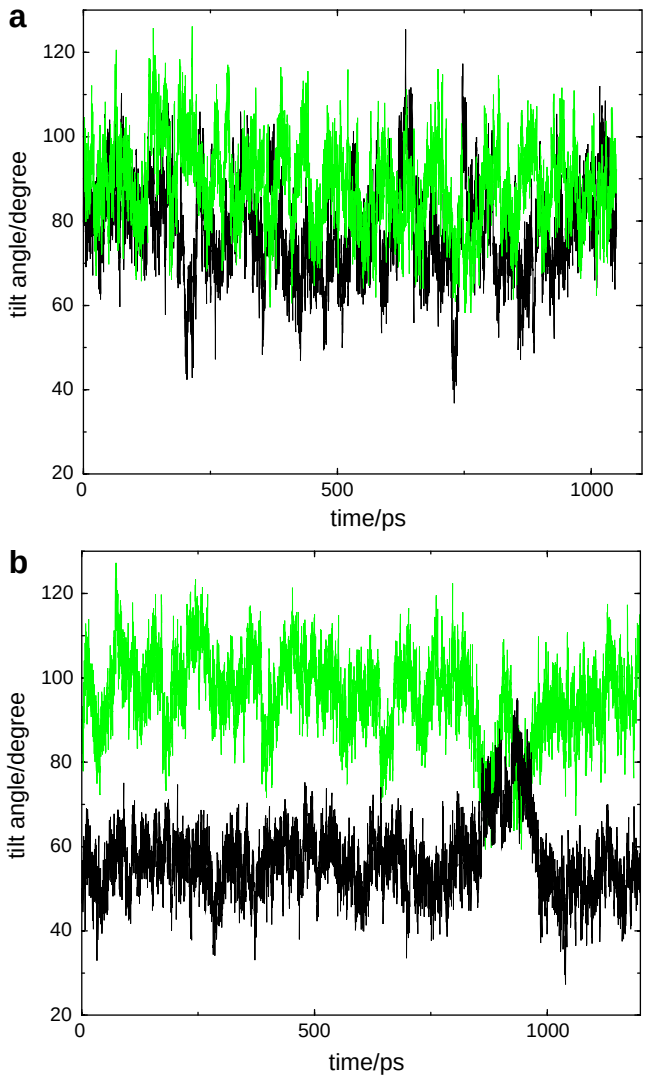

Fig. 3. Maximum and minimum variation of tilt angle, τ. **a** β-CD molecule and **b** Model A.

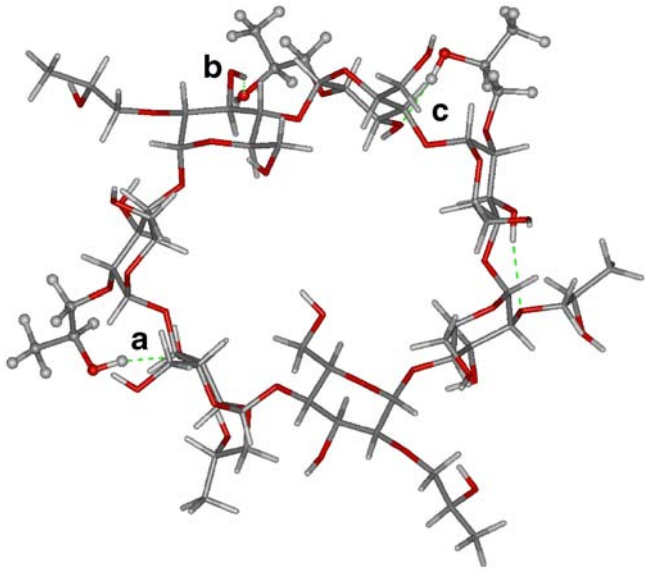

Fig. 4. Atomic configuration of Model A with water molecules removed. The 2-hydroxypropyl groups that participate in forming hydrogen bondings (labelled *a*, *b* and *c*) are highlighted in the ball and stick model.

Intramolecular Hydrogen Bondings

It is known that the intramolecular hydrogen bondings of O2–O3 is the characteristic feature of the cyclodextrin molecules. This is particular true for the β-CD, of which the stable intramolecular hydrogen bonding network gives rise to the abnormal solubility behaviour (25). Our simulation results show that the O2–O3 hydrogen bond network was disrupted in the substituted CD models. The average O2–O3 distance for β-CD is 2.89 Å, which is well within the distance to form stable hydrogen bonds. When the O2 is substituted with the 2-hydroxypropyl groups, the distance increases to more than 3.2 Å. In the case of Model D, partial substitution of 2-hydroxypropyl side group at the O2 positions still permits the O2–O3 hydrogen bond formation between the un-substituted hydroxyl groups. However, it is significantly weakened, with about three times increase in the O2–O3 distance fluctuation when compared with that of native CD.

In the case of the O6 substitutions, no intramolecular hydrogen bond can be identified. Instead, the hydroxyl alcohol groups formed preferential hydrogen bonds with water molecules located near to the cavity entrance and with water molecules located out side the CD molecules. This is discussed in more details in the next section.

The conformational behaviour differences between the side group substitutions at the O2 and O6 positions could be

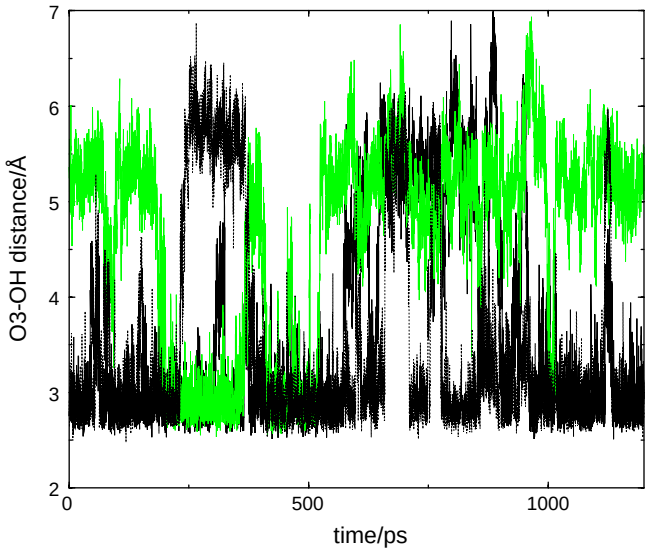

Fig. 5. Distance variation between O3 and alcohol O with respect to time. Only three (out of seven) sets of distance are shown for clarity purposes.

the results of minimising the steric effect of neighbouring bulky 2-hydroxypropyl side groups. In general, the atomic configurations show the side groups at the O2 positions are more spread out than those at the O6 positions.

In addition to the usual O2–O3 hydrogen bonds, a new set of intramolecular hydrogen bonds, formed between the hydroxyl groups at the C3 of the glucose units (see Fig. 1a) and the hydroxyl alcohol of the side chain groups (3OH–OH), was identified. This is illustrated in Fig. 4 for the atomic configuration snapshot of Model A as an example. Three such bonding network, labelled as a, b and c were shown in this example and both glucose OH and alcohol OH can act as donor and acceptor in the hydrogen bond formation. Obviously, the 3OH–OH bonding network can be disrupted due to the competitive hydrogen bond formation with the water molecules. However, simulations show that the 3OH–OH bondzing networks can be rather stable and survive up to several hundreds of picoseconds. This was determined by measuring the distance between the O3 and the hydroxyl oxygen atom of the alcohol side group, as determined by the OH–OH distance being less than 3 Å. Three sets (out of the possible seven) of such distances for the Model A are shown in Fig. 5. The other four sets of distance are not shown for clarity purposes but these distance measurements indicate the formation of the 3OH–OH hydrogen bonds most of the time during the whole simulation. All other models were also found to show similar qualitative behaviour.

Figure 5 also shows that the 3OH–OH hydrogen bonds that are broken can be reformed, and it is still possible for the side group to move completely out of the way, thus preventing the formation of the 3OH–OH hydrogen bond. One such example is shown as the green solid line in Fig. 5.

Water Interactions

The arrangement of water molecules within the cavity is determined from the cylindrical water density profile along the z-axis, with the centre of gravity of the cavity ring as the zero origin. The direction of the z-axis is perpendicular to the plane of the gycosidic oxygen atoms. This is illustrated in Fig. 6. The density profile is determined by moving an imaginary disc of radius r along the z-axis as shown in Fig. 6. The diameter r of the disc is limited to the spatial extent of the secondary O atoms from the z-axis. Thus, the density profiles obtained directly map the position of the water molecules located within and immediately outside the opening of the circular glucose units. The direction of the z-axis is such that the primary O6 groups are located in the +z region, whereas the secondary O2 groups are located at the −z region. Note that the density is measured in terms of per water molecule. This means that integration of a density profile within a given range of z distance yields the average number of water molecules within that region.

Figure 7 shows the density profiles of all the models. The vertical lines in the negative z region indicate the average distance of the secondary oxygen atoms (O2) projected along the z-axis, whereas the vertical lines in the positive z region indicate the average distance of the primary oxygen atoms (O6) projected along the z-axis. The region between these lines can be defined as the cavity size of the CD molecules. Table III shows the average number of water molecules contained in the cavities. Note that the values vary from about five to four water molecules which is lower than the estimation of previous works of about 6.5 (15). This value obviously depends on the actual definition of the cavity size. However, the results here clearly show that the nature of side chain substitution does not significantly change the occupancy of the water molecules within the cavity.

Two large density peaks, one on each side of the cavity of the β-CD model are clearly visible. These peaks are due to the hydrogen bond interactions between the water molecules, located outside the cavity entrances, and the hydroxyl groups. In the case of secondary hydroxyl groups, hydrogen bond formation with the water molecules is still rather extensive,

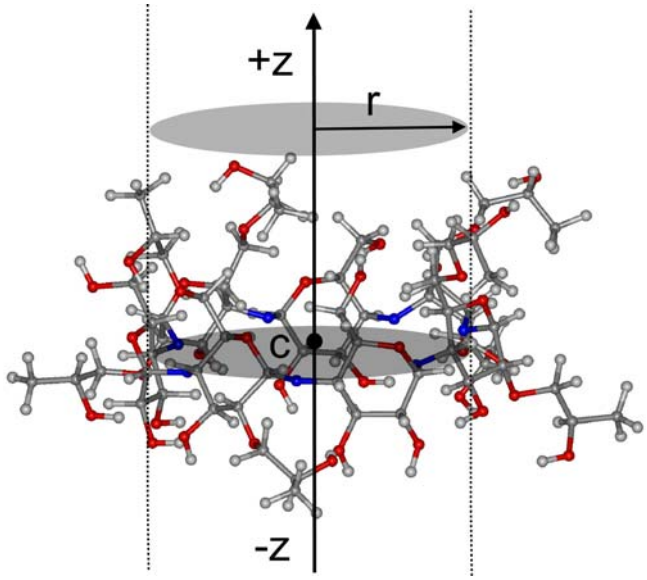

Fig. 6. Schematic diagram to illustrate the geometry for the determination of the cylindrical water density profile along the main z-axis. Point c marks the z-axis origin located at the centre of the cavity.

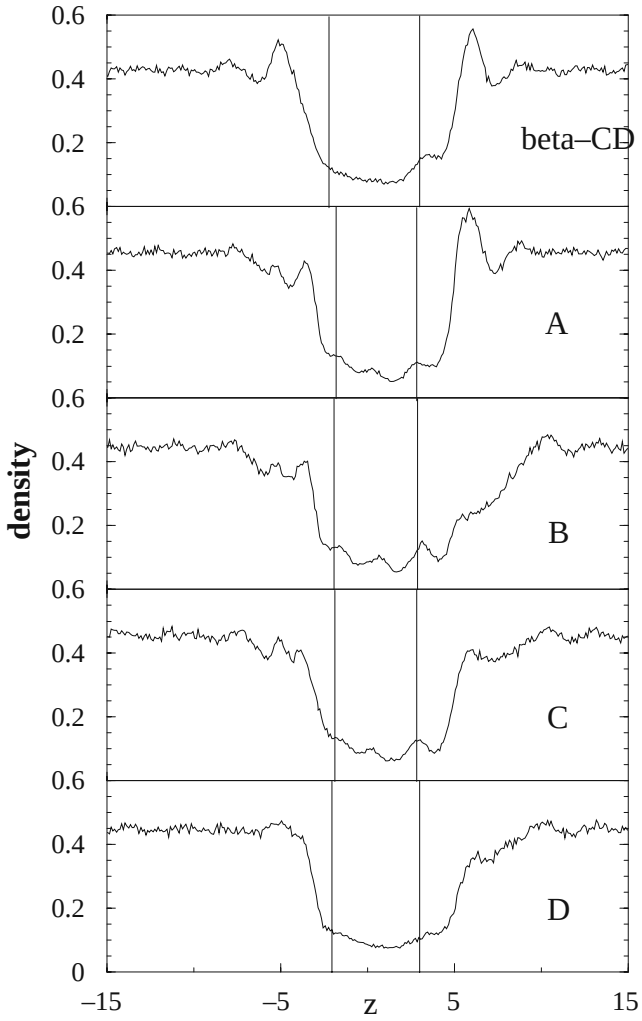

Fig. 7. Cylindrical water density profile (in unit per water molecule) across the *z*-axis (see Fig. 6 for definitions). The vertical lines indicate the average positions of the secondary oxygen atoms (negative) and the primary oxygen atoms (positive) projected along the *z*-axis.

despite the fact that the hydroxyl hydrogen atoms also involved in the intra O2–O3 hydrogen bondings. The water density at the primary O6 near the cavity (located near to the vertical line) has a higher density than that at the secondary O2 region, despite the fact that the O2 groups formed a wider cavity rim than the O6 groups. This is due to the ability of the flexible primary hydroxyl groups to form hydrogen bonds, and thus stabilise the water molecules near to the O6 cavity entrance. However, the more restricted secondary hydroxyl groups tend to form intra O2–O3 hydrogen bonds and, consequently, become less accessible to water molecules located near to the O2 cavity entrance.

The water structure is severely disrupted as the hydroxyl groups are substituted, with the disappearance of the prominent peaks in the water density profiles. The extent and nature of water structure disruptions are different between the O2 and O6 substitutions. In the case of O6 positions, the less spread-out 2-hydroxypropyl groups result in a significant reduction of the water density outside the O6 cavity. No distinct density peak and hence, ordered water structure, can be identified in this region. Due to the presence of the hydrophobic methyl groups, the hydroxyl alcohol groups become less accessible to the bulk water molecules. Instead, the hydroxyl alcohol groups formed hydrogen bonds with the water molecules at the O6 cavity entrance. Figure 8 shows a molecular configuration of Model B as an example. Only the water molecules located near and within the cavity are shown. It can be seen that flexibility of the O6 groups allows the 2-hydroxypropyl groups (highlighted as stick model in Fig. 8) to move towards the cavity and form hydrogen bonds with the water molecules located near to the primary O cavity entrance. As a result, the density peak at the O6 position is enhanced as shown for the Model B and the Model C of Fig. 7. These water molecules in turn formed hydrogen bond networks and stabilised the water molecules within the cavity. On the other hand, the two methyl groups of the side chains were orientated along the *z*-axis and over and outside the cavity entrance, thus result in the reduction of water density in the region.

In the case of the O2 positions the 2-hydroxypropyl groups adopted a more spread-out configuration, enhanced by the 3OH–OH interactions. In contrast to the O6 case, the hydroxyl alcohol can still interact directly with the water molecules located outside the O2 cavity entrance. Consequently, water density peaks, although small, are still visible outside the O2 cavity entrance (See Models A, B and C of Fig. 7). Note that the glycosidic oxygen atoms never act as a Lewis base as no hydrogen bonds with the water molecules residing in the cavity can be identified. This highlights the hydrophobic nature of the cavity.

DISCUSSION

Structural analysis of a number of 2-HPBCD molecular species shows clearly that their overall molecular structures are depended on the nature of 2-hydropropyl substitution in a rather systematic way. For instance, substitution at the O2 position results in a more "spread out" but dynamically more restricted molecular configuration. On the other hand, the 2-hydorxypropyl side groups at the O6 positions are more flexible when compare with those at the O2 positions. Such a variation in induced flexibility across different sites along the cyclodextrin molecule may have an effect on selective preference of molecular encapsulation, such as the availability of the side groups involved in the complexation process with a drug molecule.

In the case of the cyclodextrin cavity, its diameter size remains essentially unchanged. This is not surprising due to the inherent rigidity of the seven-membered glycosidic ring of the β-cyclodextrin molecule. Nevertheless, there is a noticeable

Table III. Average Number of Water Molecules Within the Cavity of the CD Molecules

Model	Number of water molecules
β-CD	4.85
A	4.18
B	4.40
C	4.43
D	4.92

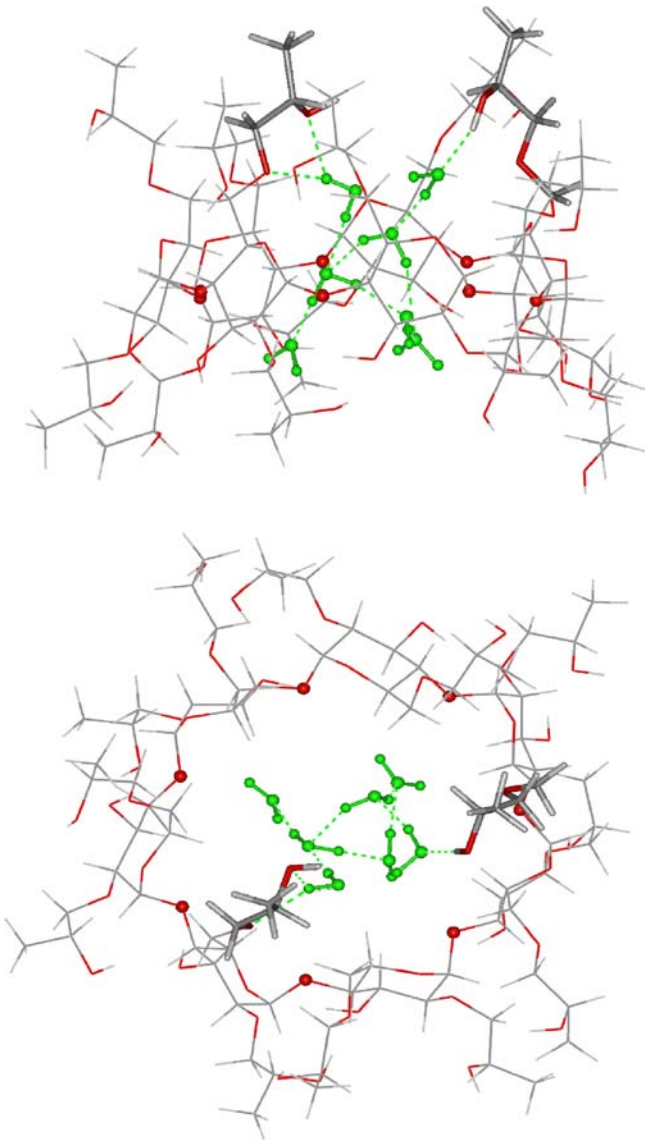

Fig. 8. '*Side*' and '*top*' view of water interactions within and near to the cavity of Model B. Only the hydrogen bonds between the water molecules and the CD molecule are shown. The 2-hydorxypropyl groups that participate in the hydrogen bond formation are highlighted as the stick model.

increase in the cavity flexibility as a result of substitution. Such effect may be an important factor in drug complexations, since these interactions are usually attractive in nature and tend to restrict the conformational freedom of the complex, leading to a negative entropy of complexation. Nevertheless, it is generally thought that van der Waals and hydrophobic interactions constitute the major driving forces for cyclodextrin complexation (26). In addition, measurements of the cavity tilt angle, τ, showed that the cavity entrance size can be changed according to both the location and extent of substitutions. In general, the O2 substitution increases the cavity entrance size as outlined by the O2 atoms but reduces the opposite end of the entrance size as outlined by the O6 atoms (see Fig. 1 for the cavity illustration). On the other hand, the opposite effect on the cavity sizes occurs for the O6 substitution. Such changes in the overall conical shape of the cavity may have a direct consequence in determining the selective nature of molecular complexation that is sensitive to the shape of the drug molecules.

Interestingly, a new set of intramolecular hydrogen bond network was identified between the hydroxyl groups of the C3 glucose unit and that of the side group, the 3OH–OH hydrogen bond network. The long-time survival of such bonding network relative to the simulation time scale means that such hydrogen bond network may play a part in restricting the motion of 2-hydroxypropyl groups and helping to maintain the molecule groups in a more spread out configuration. This consequently has a direct impact on the reductions of the tilt angle and spatial motion of the side groups as mentioned above. In addition, the density profiles showed that the 2-hydroxypropyl side groups at the O2 positions do not stabilize the water molecules located within the cavity. Instead, the flexibility of the side groups at the O6 positions allow stable hydrogen bonds to form with these water molecules.

The fact that CD molecules dissolve in water are due to the presence of polar hydroxyl groups that strongly interacting with the water molecules. However, it is known that β-CD is the least soluble among the common native cyclodextrins (25). The exact reason for such an abnormal trend is not known. One theory is that this may be due to the stable intra O2–O3 hydrogen bond network, as shown in the Fig. 1(a). This O2–O3 hydrogen bond network is unique in β-CD and enhances the rigidity of the secondary cavity rim (27) and thus, increases water structural ordering. Subsequently, there is a compensation of the favourable enthalpy by the unfavourable entropy of solution (12,25,28). In the cases of α-CD and γ-CD, the O2–O3 hydrogen bond networks are relatively insignificant due to distortions of the glycosidic ring structures.

On the other hand, the low solubility of β-CD may also be due to the unfavourable interaction of water with the β-CD that may exist as aggregates in solution bound together by a network of hydrogen bonds among the hydroxyl groups (29). Subsequently, it was found that ionisation of the hydroxyl groups leads to dispersion of these aggregates with corresponding increases in solubility (29). For this reason, derivatisation of the hydroxyl group may also help to prevent aggregation and consequently increases the CD solubility, provided the substituted groups do not interact strongly with one another. Our simulations showed that the 2-hydroxypropyl side groups adopted a more spread out configuration at the O2 positions may discourage aggregation from taking place. In addition, the results also showed that derivatisation leads to the disruption of the O2–O3 hydrogen bond network. These combining factors may be the reason for the significant increase in solubility of 2-HPBCD when compare with the native β-CD.

CONCLUSION

This study has highlighted the complex changes in structural behaviour of cyclodextrin molecules in water as a result of 2-hydroxypropyl substitutions at the O2 and O6 positions. Several intertwining factors that influence such changes have been identified. For instance, the extent and location of substitutions were found to have an effect on the structure of the cavity, in particular, the tilt angles of the glucose units. In addition, the spatial extent and flexibility of

the substituted groups also vary according to the substitution positions. A new set of intramolecular hydrogen bonding has been identified, which formed between the hydroxyl groups at the C3 of the glucose units and the hydroxyl alcohol. This type of hydrogen bonding enhances the 2-hydroxypropyl groups at the O2 positions to adopt a more spread-out configuration. On the other hand, the hydroxyl alcohol of the O6 side group formed preferential hydrogen bondings with the water molecules located near to the O6 cavity entrance.

In addition, our results also show that the overall structural behaviour of the substituted CDs also depend critically on the extent and the ratio of substitution. Obviously, these factors will have a collective direct impact on the molecular encapsulation capability. In other words, the commercially available 2-HPBCD mixture may selectively form complexes with guest molecules. This is in fact shown in other experimental work (17) as well as our study on the complexation of 9-fluorenone with 2-HPBCD (Yong *et. al.*, manuscript in preparation). Although it is not practical at present to separate the individual 2-HPBCD components from a sample mixture, this work highlights the fact that complexation behaviour may vary significantly among similar substituted 2-HPBCD isomers. Ultimately it may prove possible to use models of this type to direct the synthesis or selection of improved solubilizing agents for specific molecules.

ACKNOWLEDGEMENT

This research was carried out under a research grant from the AstraZeneca. The simulations were performed on computing resources provided by Science and Technology Facility Council's e-Science facility and HPCx, the UK's national high-performance computing service, which is provided by EPCC at the University of Edinburgh and by Science and Technology Facility Council, Daresbury Laboratory.

REFERENCES

1. J. Szejtli. *Cyclodextrin Technology*, Kluwer, Dordrecht, 1988.
2. J. Szejtli. Introduction and general overview of cyclodextrin chemistry. *Chem. Rev.* **98**:1743–1753 (1998).
3. L. Szente and J. Szejtli. Highly soluble cyclodextrin derivatives: chemistry, properties and trends in development. *Adv. Drug Delivery Rev.* **36**:17–28 (1999).
4. L. SzenteC. E. Strattan. *Hydroxypropyl β-Cyclodextrins, Preparation and Physicochemical Properties*, Edition de Santé, Paris, 1991.
5. C. J. Betlach, M. A. Gonzalez, B. C. Mckiernan, C. Neff-Davis, and N. Bodor. Oral pharmacokinetics of carbemazepine in dogs from commercial tablets and a cyclodextrin complex. *J. Pharm. Sci.* **82**:1058–1060 (1993).
6. W. Löscher, D. Hoenack, A. Richter, H. Schulz, M. Schuerer, R. Duesing, and M. E. BrewsterNew injectible aqueous carbamazepine solution through complexing with 2-hydroxypropyl-β-cyclodextrin: Tolerability and pharmacokinetics after intravenous injection in comparison to a glycofurol-based formulation. *Epilepsia.* **36**:255–261 (1995).
7. K. BLindner and W Saenger. Topography of cyclodextrin inclusion complexes. XVI. Cyclic system of hydrogen bonds: structure of α-cyclodextrin hexahydrate, form (II): comparison with form (I). *Acta Crystallogr. B.* **38**:203–210 (1982).
8. K. K. Chacko, and W. Saenger. *J. Am. Chem. Soc* **103**:1708 (1981).
9. H. –J. Schneider, F. Hacket, and V. Rüdiger. *Chem. Rev.* **98**:1755–1785 (1998).
10. N. S. Bodor, M. J. Huang, and J. D. Watts. *J. Pharm. Sci.* **84**:330 (1995).
11. C. S. Nascimento Jr., H. F. Dos Santos, and W. B. AlmeidaDe. Theoretical study of the formation of the α-cyclodextrin hexahydrate. *Chem. Phys. Lett.* **397**:422–428 (2004).
12. W. Linert, P. Margl, and F. Renz. Solute-solvent interactions between cyclodextrin and water: a molecular mechanical study. *Chem. Phys.* **161**:327–338 (1992).
13. L. Lawtrakul, H. Viernstein, and P. Wolschann. Molecular dynamics simulations of β-cyclodextrin in aqueous solution. *Int. J. Pharm.* **256**:33–41 (2003).
14. J. E. H. Koehler, W. Saenger, and W. F. Gunsterenvan. Conformational differences between α-cyclodextrin in aqueous solution and in crystalline form. *J. Mol. Biol.* **203**:241–250 (1988).
15. R. G. Winkler, S. Fioravanti, G. Ciccotti, C. Margheritis, and M. Villa. Hydration of β-cyclodextrin: A molecular dynamics simulation study. *J. Comp-Aided Mol. Design.* **14**:659–667 (2000).
16. M. Fermeglia, M. Ferrone, A. Lodi, and S. Pricl. Host-guest inclusion complexes between anticancer drugs and β-cyclodextrin: computational studies. *Carbohydr. Polym.* **53**:15–44 (2003).
17. A. Buvari-Barcza and L. Barcza. Influence of the guest, the type and degree of substitution on inclusion complex formation of substituted β-cyclodextrins. *Talanta.* **49**:577–585 (1999).
18. W. Smith, C. W. Yong, and P. M. Rodger. DL_POLY: Application to molecular simulation. *Mol. Sim.* **28**:385–471 (2002).
19. W. L. Jorgensen, J. Chandrasekhar, J. Madura, R. W. Impey, and M. L. Klein. Comparison of simple potential functions for simulating liquid water. *J. Chem. Phys.* **79**:926–935 (1983).
20. A. D. MacKerell Jr., J. Wiorkiewicz-Kuczera, and M. Karplus. An All-Atom Empirical Energy Function for the Simulation of Nucleic Acids. *J. Am. Chem. Soc.* **117**:11946–11975 (1995).
21. U. Essmann, L. Perera, M. L. Berkowtz, T. Darden, H. Lee, and L. G. Pedersen. A smooth particle mesh Ewald method. *J. Chem. Phys.* **103**:8577–8593 (1995).
22. W. Chen, C.-E. Chang, and M. K. Gilson. Calculation of cyclodextrin binding affinities: energy, entropy and implication for drug design. *Biophys. J.* **87**:3035–3049 (2004).
23. H. C. Georg, K. Coutinho, and S. Canuto. A look inside the cavity of hydrated α-cyclodextrin: A computer simulation study. *Chem. Phys. Lett.* **414**:16–21 (2005).
24. S. Melchionna, G. Ciccotti, and B. L. Holian. Mol. Phys. Hoover NPT dynamics for systems varying in size and shape. *Mol. Phys.* **78**:533–544 (1993).
25. K. J. Naidoo, J. Y. Chen, J. L. M. Jansson, G. Widmalm, and A. Maliniak. Molecular properties related to the anomalous solubility of β-cyclodextrin. *J. Phys. Chem. B.* **108**:4236–4238 (2004).
26. L. Liu and Q.-X. Guo. The driving forces in the inclusion complexation of cyclodextrins. *J. Inc. Phenom.* **42**:1–14 (2002).
27. J. E. H. Koehler, W. Saenger, and W. F. Gunsterenvan. The flip-flop hydrogen bonding phenomenon. Molecular dynamics simulation of crystalline β-cyclodextrin. *Eur. Biophys. J.* **16**:153–168 (1988).
28. E. Sabadini, T. Cosgrove, and F. do Carmo Egídio. Solubility of cyclomaltooligosaccharides (cyclodextrins) in H_2O and D_2O: a comparative study. *Carbohydr. Res.* **341**:270–274 (2006).
29. A. W. Coleman, I. Nicolis, N. Keller, and J. P. Dalbiez. Aggregation of cyclodextrins: An explanation of the abnormal solubility of β-cyclodextrin. *J. Inc. Phenom. Mol. Recog. Chemistry.* **13**:139–143 (1992).